New approach to grain fragmentation for discrete element methods

David Cantor Garcia, Nicolas Estrada, Émilien Azéma

Geomechanics from Micro to Macro – Soga et al. (Eds)
© 2015 Taylor & Francis Group, London, ISBN 978-1-138-02707-7

New approach to grain fragmentation for discrete element methods

D. Cantor & N. Estrada
Universidad de los Andes, Bogotá, Colombia

E. Azéma
Université de Montpellier 2, Montpellier, France

ABSTRACT: This article presents a new approach to grain fragmentation, its implementation in a discrete element method code, and an experimental validation. This approach is an improvement, compared with those models currently available in the literature. This new approach includes the use of polygonal particles, an estimation of stresses within the particles, a failure criterion, and a mode of rupture. The estimation of stresses is performed as a function of the forces exerted at the contacts, and the size and shape of the grains. The failure criterion is a function of the tensile strength of the material, and the mode of rupture depends on the orientation of the major principal stress. A comparison between experiments and its simulations showed a good match.

1 INTRODUCTION

Grain fragmentation is a phenomenon that can have an important effect in the mechanical behavior of granular materials. For example, it has been shown that fragmentation affects the size particle distribution (McDowell 1996, Aström 1998, Fukumoto 1992), the shear strength (Lobo-Guerrero 2006), the solid fraction (Lade 1996, Cheng 2008), and the yielding surface (Miura 1984). In addition, different industrial processes (Guimaraes 2007), and structures (Lobo-Guerreo 2005), using or built on granular materials, are also affected by grain crushing.

Although grain fragmentation has an important role, modifying the mechanical response of granular materials, only few models have been proposed to model it with discrete element methods. These models can be roughly classified into two main groups.

In the first group, the grains that satisfy certain failure condition are replaced by a set of smaller grains (Aström 1998, Lobo-Guerrero 2006, Tsoungui 1999, Buchholtz 2000). Usually, both the original grain and fragments have circular shape (Fig. 1). The main advantage of this method is its simplicity and ease to be implemented. However, it is not evident to choose the adequate number and size distribution of the fragments, and the space between fragments implies an important loss of mass.

In the second group, the grains are built as a cluster of bonded small grains (Jensen 2001, McDowell 2002, Lim 2005). The bonding strength is set-up at the beginning of the simulations, and a local criterion is responsible of determining de-bonding of the small grains, eventually leading to the division of the cluster (Fig. 2). Although this method reproduces more realistically the complex shapes of fragments after a fragmentation event, this is done at the expense of using a large quantity of grains, and, thereby, a larger computational time. Moreover, the size of the smaller grains introduces an artificial scale parameter in the system.

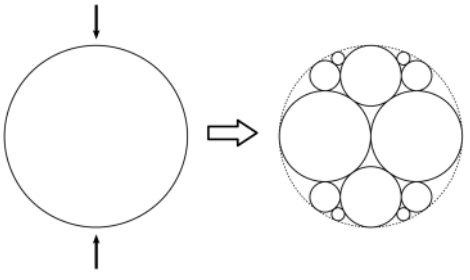

Figure 1. Example of grain fragmentation scheme following the replacement method.

Therefore, the aim of this work was to design, implement, and test a new model of grain fragmentation that allows the particles and fragments for breaking without restricting their size and shape.

This article is organized as follows. In section 2, the fragmentation model is introduced. In section 3, the physical experiments undertaken are shown. Section 4 presents the simulations results. Finally, in section 5, the conclusions are presented.

2 FRAGMENTATION MODEL

The fragmentation model is composed by three main elements: stress estimation, a failure criterion, and a fragmentation mode. These elements are detailed in the following subsections.

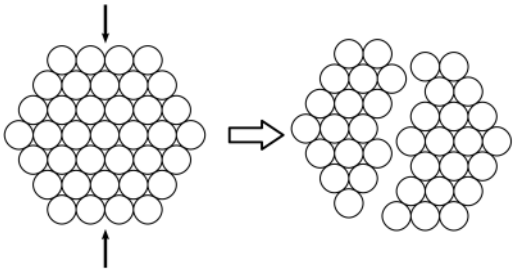

Figure 2. Example of grain fragmentation following the de-bonding method.

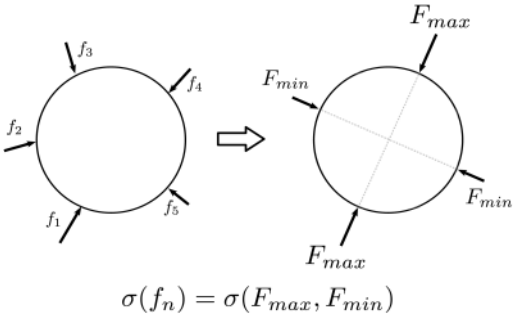

Figure 3. Reproduction of the stress tensor by means of a pair of forces applied along the principal directions.

2.1 *Stress estimation*

A grain with arbitrary shape and size, under a set of loads, presents a complex stress distribution inside it. Besides, there is not an analytical solution for this complex distribution of stresses.

So, let us first consider the case of a circular grain, for which an elastic solution of stresses exists. Given any set of loads over a circular grain, it is possible to calculate its stress tensor as follows (Moreau, 1997):

$$\boldsymbol{\sigma}_{ij} = \frac{1}{V}\sum_{c=1}^{Nc} \boldsymbol{l}_i \boldsymbol{F}_j \tag{1}$$

where V is the volume of the grain (in the two dimensional case $V = \pi R^2$, being R the radius of the particle), Nc is the number of contacts c, $\mathbf{l}$ is the branch vector between the particles in contact, and $\mathbf{F}$ is the vector of contact forces. The eigenvalues and eigenvector of $\boldsymbol{\sigma}_{ij}$ are the principal stresses and directions, respectively. Henceforward in this article, the major principal stress is called $\boldsymbol{\sigma}_{max}$ and the minor principal stress is called $\boldsymbol{\sigma}_{min}$.

From the principal stresses, it is possible to calculate a pair of equivalent forces, which, applied along the principal directions, reproduce the tensor $\boldsymbol{\sigma}$ (Fig. 3). These forces, here termed F_{max} and F_{min}, are given by

$$F_{max} = \frac{\sigma_{max}\pi r}{2} \tag{2}$$

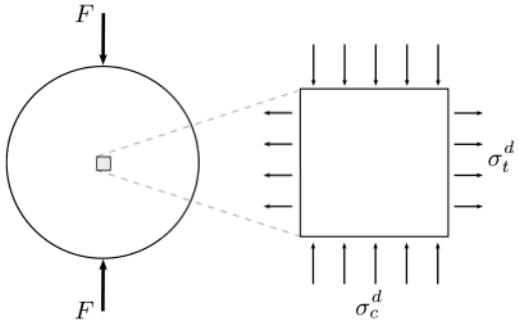

Figure 4. Tensile and compression stresses at the center of the particle, produced by a diametrical load.

and

$$F_{min} = \frac{\sigma_{min}\pi r}{2} \tag{3}$$

If it is assumed that the grain is made of a brittle material that deforms elastically, it is known that these forces generate compression stresses along their direction of action and tensile stresses in the orthogonal direction (Fig. 4). Given that the tensile stress controls the failure of brittle materials (Engelder 1974, Sammis 1987), its maximum value can be estimated as the superposition of the tensile stress produced by σ_{max} (4) and the compression stress produced by σ_{min} (5). In this article, the maximum tensile stress is called the net tensile stress for discs (6):

$$\sigma_t^d = \frac{F_{max}}{\pi R} \tag{4}$$

$$\sigma_c^d = \frac{3F_{min}}{\pi R} \tag{5}$$

$$\sigma_{t_{net}}^d = \frac{F_{max}}{\pi R} - \frac{3F_{min}}{\pi R} \tag{6}$$

Note that the tensile stress (4) is calculated at the center of the grain, where its value is maximum, and the compression stress (5) is calculated at the same location.

However, as it was mentioned in the previous paragraphs, the precedent calculation of stresses is only valid for circular grains. For different grain shapes, a correction must be introduced.

In order to find the adequate correction, a series of numerical tests were performed by means of the finite element software ABAQUS, using the linear elastic material behavior, an elastic modulus of 21GPa, and a Poisson's ratio of 0.3.

In these tests, a set of grains of unit area and different shapes were loaded diametrically with a unit load.

Figure 5 shows the tensile stresses distribution in some of the polygonal shapes that were tested. For each of these tests, it was found that the maximum tensile stress was near the center of mass of the grains

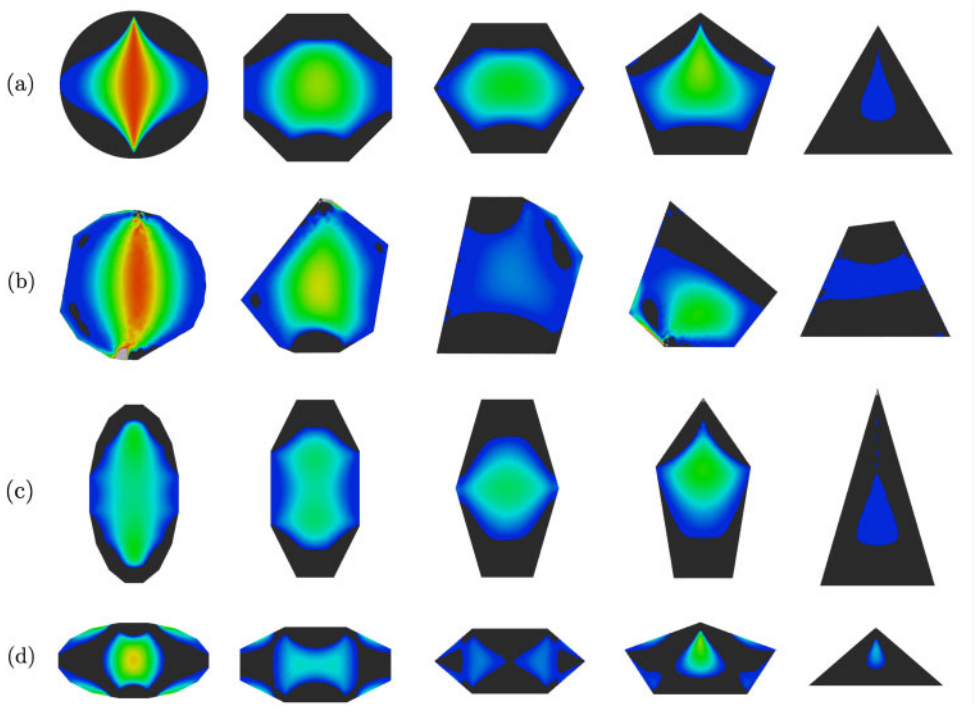

Figure 5. Tensile stress distribution for (a) regular, (b) irregular, (c) vertically elongated, and (d) horizontally elongated grains under unit vertical load.

and its direction was almost orthogonal to the unit load. Then, for each grain the compression stress in the same location as the maximum tensile stress was measured.

Figure 6 shows the magnitudes of the maximum tensile stress σ_t and the compression stress σ_c, measured in each polygon, as functions of a dimensionless parameter $\bar{l}/w$, where $\bar{l}$ is the mean length of the sides intersected by the load direction, and w is the particle width (see inset in Fig. 6 for a graphical explanation).

It can be seen that σ_t decreases from ~0.6 to 0, and σ_c varies between ~2 and 1. Note that these values correspond to those of a circle and a square, respectively. Thus, despite de dispersion of the data points, a simple way to estimate σ_t and σ_c for any polygonal shape, is to consider a linear function that joins the data points for the circle and the square (i.e. dashed lines in figure 6). This approach leads to the following equations:

$$\sigma_t = \sigma_t^d \left(1 - \frac{\bar{l}}{w}\right) \tag{7}$$

$$\sigma_c = \sigma_c^d \left(1 - \frac{\bar{l}}{w}\right) - \frac{\bar{l}F}{w^2} \tag{8}$$

where σ_t^d and σ_t^d are given by equations 4 and 5, considering a disc of the same area as the polygon. Finally,

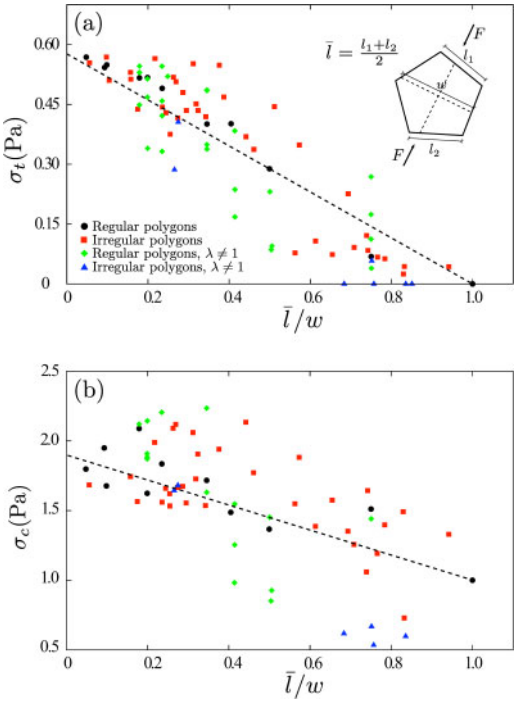

Figure 6. (a) Maximum tensile stress and (b) compression stress at the same location measured in the finite element tests.

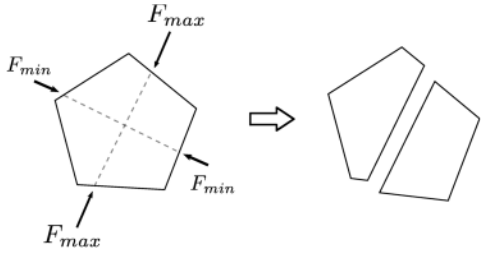

Figure 7. Schematic representation of the fragmentation mode.

after superposing both stresses, the net tensile stress for the polygon can be written as

$$\sigma_{t_{net}} = \frac{F_{max}}{\pi R}\left(1 - \frac{\bar{l}_{max}}{w_{max}}\right) - \frac{3F_{min}}{\pi R}\left(1 - \frac{\bar{l}_{min}}{w_{min}}\right) + \frac{\bar{l}_{min}F_{min}}{w_{min}^2} \quad (9)$$

where the subscript "max" refers to those values calculated from the maximum principal stress value and orientation, and the subscript "min" refers to those based on the minor principal stress and orientation.

2.2 *Failure criterion*

The failure criterion determines the stress condition for which a grain must be fragmented. As it was mentioned in the previous subsection, the tensile stresses are the principal responsible for this phenomenon. For this reason, in this model, the fragmentation of a grain occurs when the net tensile stress of the particle equals or surpasses the tensile strength of the material σ_{crit}. This means that, if

$$\sigma_t \geq \sigma_{crit} \quad (10)$$

then the grain must break. Notice that σ_{crit} is the only parameter this model requires, and its value can be found through the indirect tensile test, also known as the Brazilian test.

2.3 *Fragmentation mode*

The fragmentation mode determines the way in which the grains break once the failure criterion is satisfied. In this model, the original grain splits up in two segments defined by a line that, having the orientation of the major principal stress, passes through the center of mass of the particle. A scheme of this fragmentation mode is presented in Figure 7.

3 EXPERIMENTS

In order to validate the model, a set of experiments was undertaken. For these tests, the material used was powder plaster given its ease to be molded and its brittle behavior. First, a number of diametrical load tests were conducted to find the tensile strength of the material. Then, four oedometric compression tests were carried out over a system of several grains. The results of these experiments are presented in the following subsections.

3.1 *Tensile strength of the material*

Twelve circular particles were built in plaster, under controlled conditions of temperature, amounts of water, and drying time. The particles had a thickness t_d, of 6 mm and a diameter that varied between 1 and 3 cm. Then, these particles were brought to failure in diametrical compression tests.

Figure 8 shows a close up of the loading device and the corresponding photographs of the particles after the test. This device allowed for measuring the vertical load at failure (F_{crit}), and, consequently, the tensile strength of the material, calculated as

$$\sigma_{crit} = \frac{F_{crit}}{\pi R t_d} \quad (11)$$

The average tensile strength of the material was 800 kPa.

3.2 *Oedometric compression tests*

Using the material previously described, a set of polygonal particles was built. The circum diameter of the particles varied between 1 and 3 cm, and their thickness was 6 mm. Using these particles, four different systems of 15 disordered particles were built inside a Plexiglas box. These systems were oedometrically compressed in plane strain conditions, at a constant velocity of 1 mm/min.

4 SIMULATION AND MODEL VALIDATION

The simulation of the oedometric tests was carried out using the contact dynamics method (Moreau 1994, Jean 1995, Radjaï 2011). This numerical method assumes perfectly rigid particles interacting through mutual exclusion and Coulomb's friction. The friction between the particles, and between the particles and the Plexiglas box was measured in laboratory resulting in 0.70, and 0.78 respectively.

The initial distribution of particles was numerically replicated, and the boundary conditions were set up. The deformation advanced, in both the experiment and the simulation, with the same velocity until a vertical strain of 10%.

Figure 9 shows a qualitative comparison between one of the experiments and its corresponding simulation. From these images, it can be observed that the match is good in terms of the grains that break, the order of occurrence, and the directions of the cracks. It should be remarked that this comparison is made

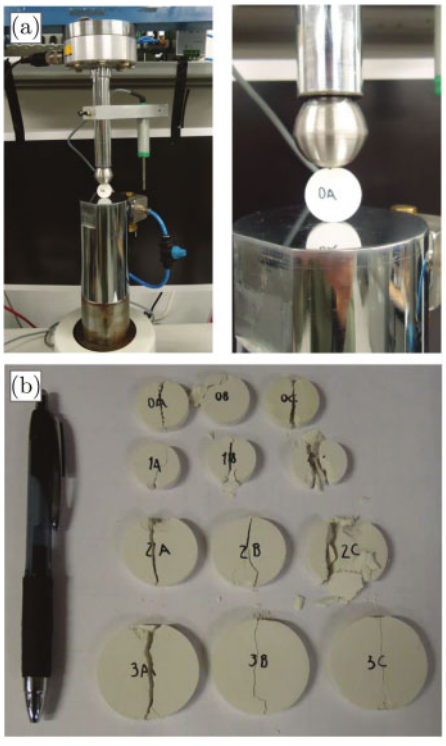

Figure 8. Pictures of (a) the loading device, and (b) the particles after the compression tests.

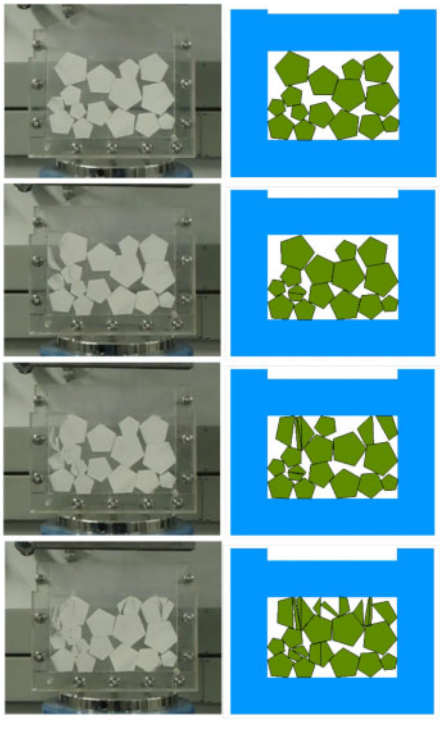

Figure 9. Qualitative comparison between the experiment and the simulation.

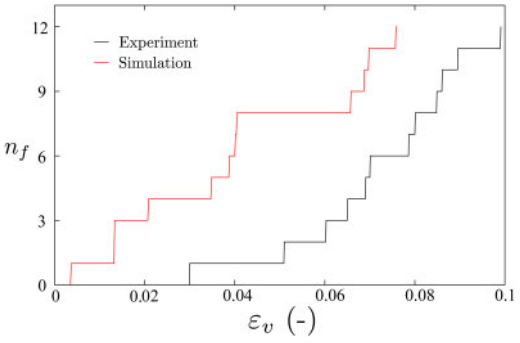

Figure 10. Number of fragmentation events as function of the vertical strain in both the experiment and simulation.

in terms of equivalent fragmentation states, but the strain levels do not necessarily correspond. In general, the fragmentation events occurred earlier in the simulations that in the experiments.

Figure 10 shows the cumulative fragmentation events as a function of the vertical strain (ε_v), for both the experiment and simulation presented in Fig. 9.As it can be seen, there is a strain gap between the fragmentation events.

This difference or gap, observed in Figured 10, can be explained since the contact dynamics assumes perfectly rigid particles, and the experimental test deforms elastically. Thus, the forces exerted in the contacts between particles increase more rapidly in the simulations, and, consequently, the fragmentation events occur earlier.

5 CONCLUSIONS

This paper presents a new method for implementing grain fragmentation in a discrete element code. The proposed approach reproduces more adequately the shape and size of the fragments, conserves the mass after each fragmentation event, and does not introduce unclear variables into the system.

The approach can be understood as a combination of three principal elements: stress estimation, a failure criterion, and a mode of rupture. The stress estimation resulted from a stress analysis undertaken in a finite element software, and the criterion and mode of rupture are consequence of field and practical observations.

In order to validate the numerical model, a set of experiments was performed. Four different systems made up of polygonal particles were placed in a Plexiglas box and compressed oedometrically. A qualitative comparison between the experiments and the respective simulations showed a good match in terms of particles that break, sequence of fragmentation, and direction of the cracks.

Additionally, a quantitative comparison was made in terms of fragmentation occurrence as a function of the vertical strain. This comparison showed a continual difference between the strain levels at which

fragmentation events occur in the experiments and the simulations. In one part, this difference can be explained by the fact that the discrete element method that was used assumes perfectly rigid particles, and disregards the elastic deformation of the particles. In other part, it should be remarked that the systems tested were small, and minor differences in the initial geometry of the sample, the evolution of fragmentation events, or the boundary conditions can have important effects in the results.

Evidently, grain fragmentation is a complex phenomenon that is only partially captured by a numerical model such as the one presented in this article. However, this model is an important advance in order to improve the way fragmentation is simulated in discrete element methods.

Future studies can be focused on additional quantitative comparisons with larger granular samples, on the shear resistance-strain effect, and on the use of more complex particles shapes, such as spheropolygons.

ACKNOWLEDGEMENTS

We thank in particular Alfredo Taboada and Farhang Radjaï for fruitful discussions. We also acknowledge financial support by the Ecos-Nord program (Grant No. C12PU01).

REFERENCES

Aström, J. & Herrman, H. 1998. Fragmentation of grains in a two-dimensional packing. *The European Physical Journal B* (5): 551–554.

Buchholtz, V. Freund, J. & Pöschel, T. 2000. Molecular dynamics of comminution in ball mills. *The European Physical Journal B* (16): 169–182.

Cheng, Y., Nakata, Y. & Bolton, M. 2008. Micro- and macro-mechanical behaviour of DEM crushable materials. *Géotechnique* (58): 471–480.

Engelder, J. 1974. Cataclasis and the generation of fault gouge. *Geol. Soc. Am. Bull*. (85): 1515–1522.

Fukumoto, T. 1992. Particle breakage characteristics of granular soils. *The Japanese Geotechnical Society* (32): 26–40.

Guimaraes, M., Valdes, J., Palomino, A. & Santamarina, J. 2007. Aggregate production: Fines generation during rock crushing. *International Journal of Mineral Processing* (81): 237–247.

Jean, M. 1995. *Mechanics of Geometrical Interfaces*. New York: Elsevier.

Jensen, R. & Plesha, M. 2001. DEM simulation of particle damage in granular media-structure interfaces. *International Journal of Geomechanics* (1): 21–39.

Lade, P., Yamamuro, J. & Bopp, P. 1996. Significance of particle crushing in granular materials. *Journal of Geotechnical Engineering* (122): 309–316.

Lim, W. & McDowell, G. Discrete element modelling of railway ballast. *Granular Matter* (7): 19–29.

Lobo-Guerrero, S. & Vallejo, L. 2005.DEM analysis of crushing around driven piles in granular materials. *Géotechnique* (55): 617–623.

Lobo-Guerrero, S. 2006. Visualization of crushing evolution in granular materials under compression using DEM. *International Journal of Geomechanics* (6): 195–200.

McDowell, G., Bolton, M. & Robertson, D. 1996. The fractal crushing of granular materials. *Journal of the Mechanics and Physics of Solids* (44): 2079–2101.

McDowell, G. & Harireche, O. 2002. Discrete element modelling of soil particle fracture. *Géotechnique* (52): 131–135.

Miura, N., Murata, H. & Yasufuku, N. Stress-strain characteristics of sand in a particle-crushing region. *Soils and Foundations* (24): 77–89.

Moreau, J.J. 1994. Some numerical methods in multibody dynamics: Application to granular materials. *European Journal of Mechanics, A/Solids*. (13 Suppl): 93–114.

Moreau, J.J. 1997. *Friction, Arching, Contact Dynamics*. Singapore: World Scientific.

Radjaï, F. & Dubois, F. 2011. *Discrete-element modeling of granular materials*. ISTE Ltd. and John Wiley \& Sons, Inc.

Sammis, C., King, G. & Biegel, R. 1987. The kinematics of gouge deformation. *Pure and Appl. Geophys*. (125): 777–812.

Tsoungui, O., Vallet, D. & Charmet, J. Numerical model of crushing of grains inside two-dimensional granular materials. *Powder technology* (105): 190–198.